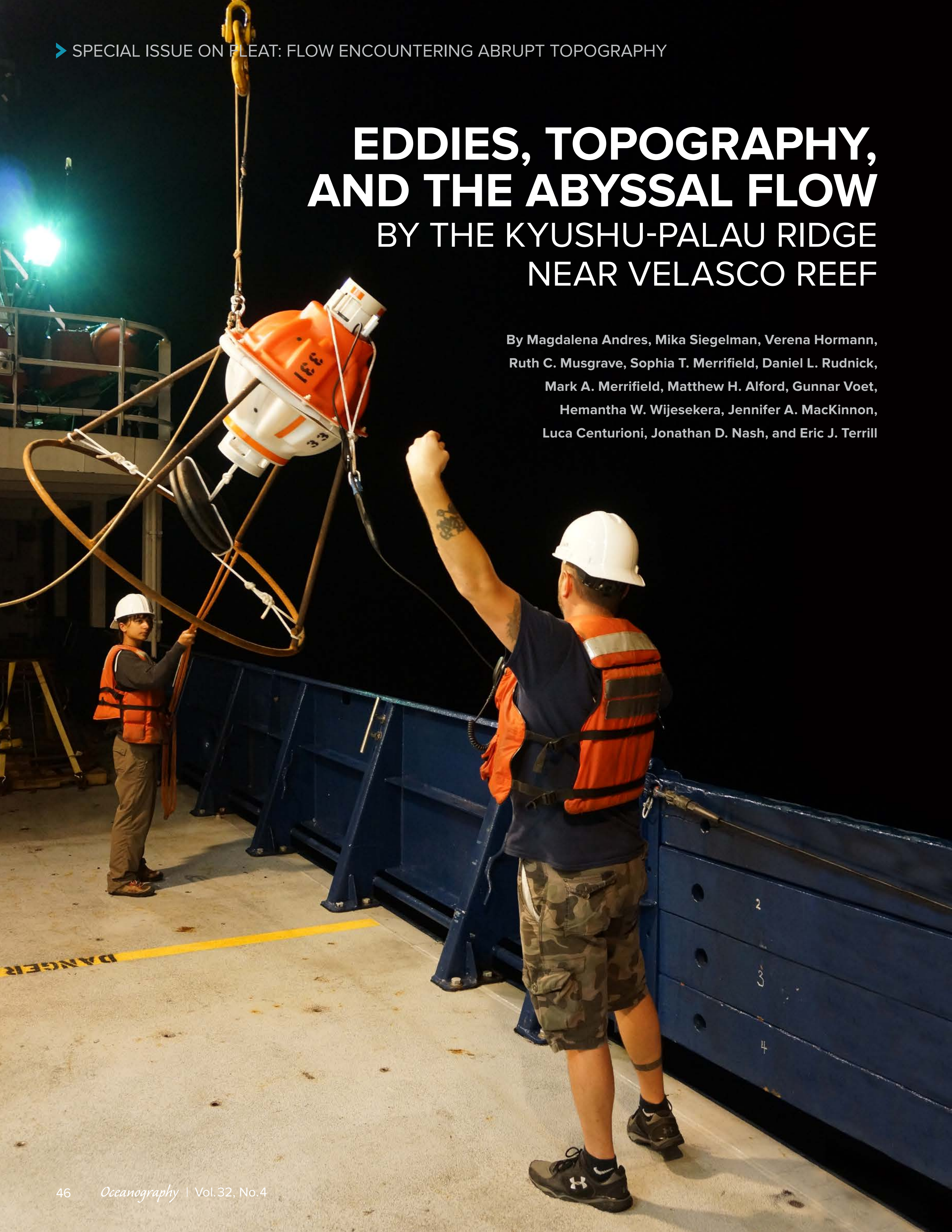

EDDIES, TOPOGRAPHY, AND THE ABYSSAL FLOW
BY THE KYUSHU-PALAU RIDGE NEAR VELASCO REEF

By Magdalena Andres, Mika Siegelman, Verena Hormann, Ruth C. Musgrave, Sophia T. Merrifield, Daniel L. Rudnick, Mark A. Merrifield, Matthew H. Alford, Gunnar Voet, Hemantha W. Wijesekera, Jennifer A. MacKinnon, Luca Centurioni, Jonathan D. Nash, and Eric J. Terrill

> "Understanding nearly geostrophic flow and what happens to its vertical structure when it encounters topography is a major goal of the Flow Encountering Abrupt Topography (FLEAT) program..."

ABSTRACT. Palau, an island group in the tropical western North Pacific at the southern end of Kyushu-Palau Ridge, sits near the boundary between the westward-flowing North Equatorial Current (NEC) and the eastward-flowing North Equatorial Countercurrent. Combining remote-sensing observations of the sea surface with an unprecedented in situ set of subsurface measurements, we examine the flow near Palau with a particular focus on the abyssal circulation and on the deep expression of mesoscale eddies in the region. We find that the deep currents time-averaged over 10 months are generally very weak north of Palau and not aligned with the NEC in the upper ocean. This weak abyssal flow is punctuated by the passing of mesoscale eddies, evident as sea surface height anomalies, that disrupt the mean flow from the surface to the seafloor. Eddy influence is observed to depths exceeding 4,200 m. These deep-reaching mesoscale eddies typically propagate westward past Palau, and as they do, any associated deep flows must contend with the topography of the Kyushu-Palau Ridge. This interaction leads to vertical structure far below the main thermocline. Observations examined here for one particularly strong and well-sampled eddy suggest that the flow was equivalent barotropic in the far field east and west of the ridge, with a more complicated vertical structure in the immediate vicinity of the ridge by the tip of Velasco Reef.

INTRODUCTION: AN EDDY SOUP IN THE PACIFIC

In nearly geostrophic flows, horizontal currents are supported by a first-order balance between Coriolis and pressure gradient forces. In the western North Pacific, these flows include not only large-scale currents like the North Equatorial Current (NEC) and the North Equatorial Countercurrent (NECC), but also smaller, mesoscale features. At low latitudes, mesoscale eddies—coherent vortices of clockwise or counterclockwise swirling water—are typically several hundred kilometers in diameter and manifest as closed contours of high (anticyclonic) and low (cyclonic) sea surface height (SSH).

These nonlinear mesoscale eddies, or ocean storms, are ubiquitous in satellite-derived SSH maps and fill much of the North Pacific Ocean away from the equator (Chelton et al., 2011). In the low-latitude western North Pacific along 8.5°N, cyclonic and anticyclonic eddies are generated near or west of the dateline (e.g., Schönau et al., 2019, in this issue). Consecutive maps of SSH anomalies (SSHa) from satellite altimetry show that many of these eddies move westward (**Figure 1**) and eventually approach Palau, where they interact with the islands and the surrounding subsurface plateaus and ridges.

A mesoscale eddy's vertical structure (i.e., the depth to which the swirling horizontal currents extend in the water column beneath its SSH signature) depends on the three-dimensional pressure field, which in turn is dictated by the density field. Idealized ocean models that are simplified to 1½ (or 2½) layers may predict the westward propagation of these eddies across ocean basins reasonably well, but they completely miss the deep ocean part of the story. These models limit eddy expression to the upper layers; the model's "½ layer" on the bottom, which is infinitely thick, is at rest. This is a poor representation of the real ocean's lower layer, which not only is finite and moving but also is littered with complicated mid-basin topography. Little is known about the vertical reach of mesoscale eddies in the open ocean, in part due to limited in situ observations below 2,000 m. Hence, their interactions with abrupt topography and the consequent coupling between lower- and upper-ocean flows are often ignored. Understanding nearly geostrophic flow and what happens to its vertical structure when it encounters topography is a major goal of the Flow Encountering Abrupt Topography (FLEAT) program, sponsored by the US Office of Naval Research.

Eddies' surface expressions have been relatively well studied with altimetry, and the global Argo profiling float program has provided complementary informa-

FACING PAGE. A pressure-sensing inverted echo sounder (PIES) is deployed from R/V *Roger Revelle* as part of the Flow Encountering Abrupt Topography (FLEAT) Array north of Velasco Reef. The instrument array was in the water for 10 months. *Photo credit: T. Peacock* tion about their subsurface expressions in the thermocline (e.g., Zhang et al., 2014). Moored arrays have also been used to examine the subsurface expressions of eddies associated with SSHa that passed by the fixed instruments (e.g., Ramp et al., 2017). In the North Pacific, where these westward-propagating eddies eventually impinge on the western boundary currents, eddy-Kuroshio-topography interactions have been explored recently with in situ observations and numerical models (e.g., Jan et al., 2017, and Yan et al., 2019). However, eddy deep vertical structure in the open ocean near mid-basin topography is particularly poorly characterized.

This knowledge gap is important to address as human activity in the deep ocean—related, for example, to deep sea mining or oil extraction—increases. Deep currents associated with the passage of these mesoscale eddies may affect dispersal of suspended sediments associated with mining operations (Aleynik et al., 2017). Further, the interactions of deep-reaching eddies with topography may also play an important role in the dissipation of mesoscale energy as eddies decay (Sekine, 1989; Zhang et al., 2016; Yang et al., 2019). Here, we use in situ data from the FLEAT field program focused near Palau—together with satellite altimetry that provides the broader spatial context about the upper ocean—to examine the mean abyssal flows north of Palau and to explore the interactions of mesoscale eddies with the topography there.

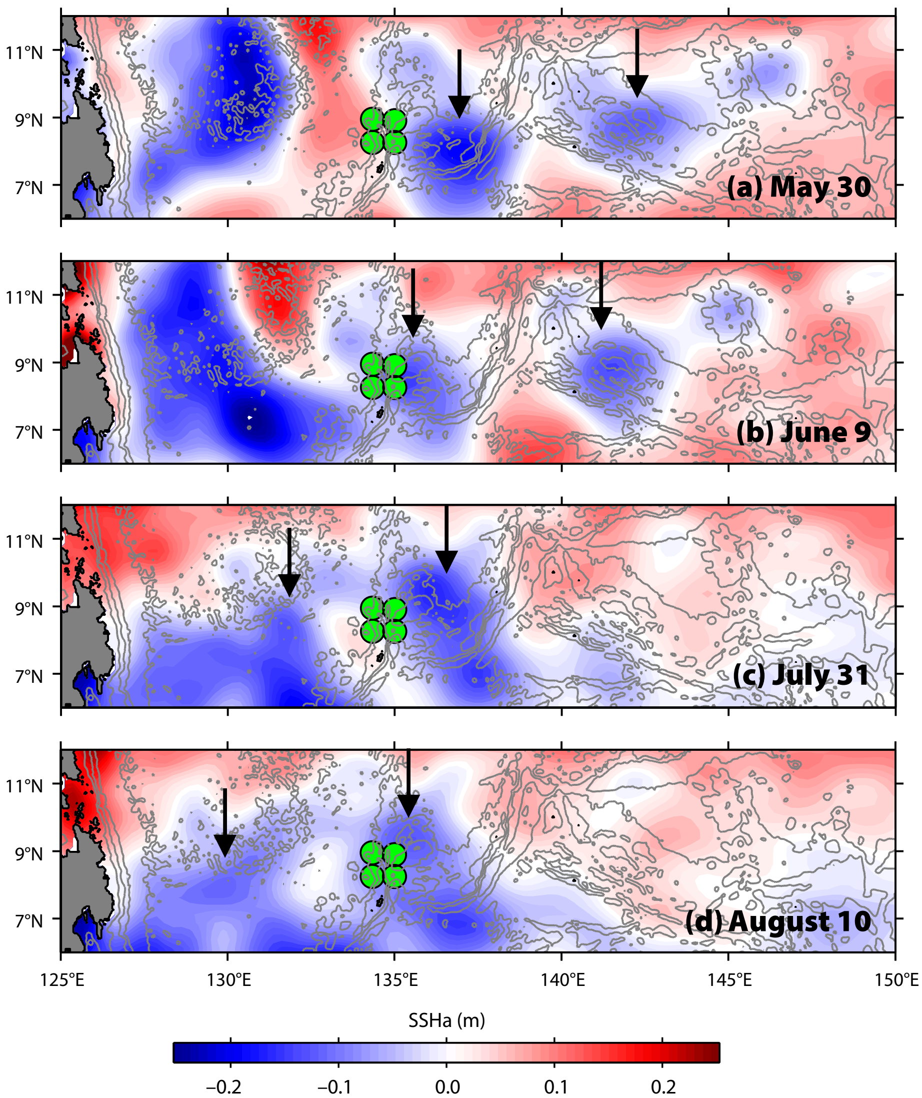

FIGURE 1. Maps of sea surface height anomaly (SSHa) around Palau from satellite altimetry. In each daily map, the area-averaged SSH from altimetry (132°–155°E, 6°–12°N) has been subtracted from the total mapped absolute dynamic topography (MADT) at each grid point to produce the anomaly maps. Arrows highlight two SSHa lows that are further examined here with in situ observations. These two features move westward at roughly 10 km day^{-1}. Bathymetry is contoured at 1,000 m intervals to 6,000 m depth (gray). Green dots show the locations of the four current- and pressure-sensing inverted echo sounders (CPIESs) north of Palau. The Philippines are visible at the western boundary.

IN SITU OBSERVATIONS: A WINDOW INTO THE ABYSS NEAR PALAU

The FLEAT Array

Through FLEAT, an array of instruments (Table 1) was deployed from May 2016 through April 2017 north of Palau surrounding Velasco Reef near the southern end of the Kyushu-Palau Ridge (Figure 2a). These in situ data provide direct measures of the abyssal circulation and the subsurface expression of several westward-propagating cyclonic mesoscale eddies near Palau. The deepest measurements of currents made by the array came from four current- and pressure-sensing inverted echo sounders (CPIESs, green circles) that were deployed on the seabed surrounding the Kyushu-Palau Ridge at depths between 2,600 m and 4,300 m (C3, C5, C7, and C8) and from three tall moorings (large yellow triangles), deployed on the western flank of the ridge on isobaths ranging from 3,400 m to 1,500 m (F1–F3, with the ridge crest just east of F3 reaching to about 950 m). These deep velocity measurements are used here to examine the mean and time-varying near-bottom currents during the 10-month deployment period. Measurements from two additional shallower moorings (F4 and F6, small white triangles), which were focused on the upper ocean at the tip of Velasco Reef, are used here with other in situ and remote-sensing observations to examine the interaction with the Kyushu-Palau Ridge of a cyclonic eddy that crossed the FLEAT Array early during the 10-month deployment period.

The in situ FLEAT measurement records used here include the following. At each CPIES site, a current meter measured hourly the horizontal currents 50 m above the bottom with an Aanderaa Z-pulse 4390R sensor tethered to the main body of the CPIES instrument. In addition, the CPIESs made hourly measures of the bottom pressure and the round trip surface-to-bottom acoustic travel time, which is an integrated measure related to the temperature and salinity profile of the overlying water column (Watts and Rossby, 1977).

The tall and shallow moorings consisted of thermistors, conductivity-temperature-depth sensors (CTDs), and acoustic Doppler current profilers (ADCPs). At each tall-mooring site (large yellow triangles), nearly full-depth velocity measurements were achieved by deploying as many as five 75 kHz or 300 kHz ADCPs distributed throughout the water column. Typically, the 75 kHz ADCPs had a sampling period of either 15 or 30 minutes and a bin size of 16 m. The 300 kHz ADCPs had a shorter sampling period of 6 minutes and a bin size of 4 m. The shallow moorings (small white triangles) comprised an upward-looking 300 kHz and a downward-looking 75 kHz ADCP and recorded velocity in the upper 600 m of the water column. The 300 kHz ADCP sampled every 20 minutes with a 4 m bin size, and the 75 kHz ADCP sampled every hour with an 8 m bin size.

> "Eddy deep vertical structure in the open ocean near mid-basin topography is particularly poorly characterized. This knowledge gap is important to address as human activity in the deep ocean—related, for example, to deep-sea mining or oil extraction—increases."

Context for the FLEAT Array

In addition to these fixed assets, Spray gliders and satellite-tracked drifters drogued at 15 m depth sampled the region surrounding the FLEAT Array, spanning a longer time period than the in situ array. Since October 2015, more than 100 Surface Velocity Program (SVP) drifters have been deployed in the area, providing Lagrangian velocity and sea surface temperature (SST) as well as optional sea level pressure (SLP) observations with nominal hourly resolution; additional information on the FLEAT drifter experiment can be found in Paluszkiewicz et al. (2019, in this issue). Details of the Spray glider missions are included in Rudnick et al. (2019, in this issue).

TABLE 1. FLEAT Array instrument locations and the observed near-bottom, time-averaged flow.

Site ID[1]	Instrument Type	Latitude (°N)	Longitude (°E)	Water Depth (m)	$<u_{bot}>$ (cm s^{-1})	mse[2] (cm s^{-1})	$<v_{bot}>$ (cm s^{-1})	mse[2] (cm s^{-1})	Bottom Speed[3] (cm s^{-1})
C3	CPIES	8°14.978'	134°19.887'	4,283	0.2	0.7	–0.1	0.7	0.3
C5	CPIES	8°57.029'	134°19.839'	4,157	–0.0	0.3	–0.7	0.4	**0.7**
C7	CPIES	8°54.009'	134°59.924'	3,054	0.3	0.3	0.2	0.4	**0.4**
C8	CPIES	8°15.318'	135°00.005'	2,621	1.4	0.2	–0.4	0.1	**1.4**
F1	Mooring	8°40.838'	134°24.087'	3,390	0.1	0.1	–1.8	0.6	**1.8**
F2	Mooring	8°30.164'	134°35.532'	1,515	0.5	0.1	–0.1	0.1	**0.5**
F3	Mooring	8°32.718'	134°37.414'	1,666	0.4	0.3	0.0	0.5	**0.4**
F4	Mooring	8°29.862'	134°38.723'	1,515	–	–	–	–	–
F6	Mooring	8°28.962'	134°38.574'	434	–	–	–	–	–

[1] The islands comprising Palau sit in a "diamond" between neighboring altimeter tracks. C5 and C7 were situated directly on tracks (the satellite's repeat sampling along a track is about 10 days).

[2] Mean standard errors (mse) for each time-averaged velocity component are calculated with the time-series' equivalent degrees of freedom computed from the decorrelation timescales, which are in turn estimated from the first zero-crossings in autocorrelation plots for each velocity component.

[3] If the mse is greater than the magnitude of the time-averaged velocity component, the mean is not significantly different than zero flow. Those sites with statistically significant non-zero mean bottom speeds are in bold type (i.e., these are the sites where at least one component of the time-averaged flow is significantly different than 0 cm s^{-1} as indicated by comparing the respective mse to $<u_{bot}>$ and $<v_{bot}>$).

To provide spatial and temporal context for the FLEAT measurements, we use SSH and the derived near-surface geostrophic velocities (u, v) from the daily mapped reference product provided by AVISO. To further examine the arrival of one cyclonic eddy at Palau, we compare these satellite-derived velocities to velocities from three HF radar systems that were installed in 2016 at Kayangel (a small atoll north of the largest island), Melekeok (the largest island), and Angaur (a small island to the south) as part of the FLEAT program (Figure 2a, magenta squares). These provided hourly, 6 km resolution surface currents on the north and east sides of Palau (Merrifield et al., 2019, in this issue).

THE STEADY FLOW INFERRED FROM OBSERVATIONS

Using the deepest available current records, we find that the time-averaged near-bottom velocities ($\langle u_{bot} \rangle$, $\langle v_{bot} \rangle$) are very close to zero everywhere (Table 1). The strongest mean flows observed are the east-southeastward flow (1.4 cm s^{-1}) at C8 and southward flow (1.8 cm s^{-1}) at F1 (Figure 2a). Except at the two sites on the northwestern edge of the array (C5 and F1), the mean flows have an eastward component. This eastward component is statistically different than zero mean (with significance established by examining the mean standard error; see the footnotes to Table 1), except at C3 where the variability is large in comparison to the mean.

This eastward component of the time-averaged near-bottom flows is opposite the NEC, which generally flows westward across the Kyushu-Palau Ridge as reported by Schönau and Rudnick (2015) and inferred here from the SSH isopleths and a few representative drifter tracks (Figure 3). The NEC is observed both during the El Niño just prior to the FLEAT Array deployment period and during the subsequent La Niña. Near-surface geostrophic flows are along SSH isolines, with the fastest flow coinciding with the strongest SSH gradients. Despite the overall lower SSH in the western North Pacific during the El Niño (Figure 3a and b, shading), which is

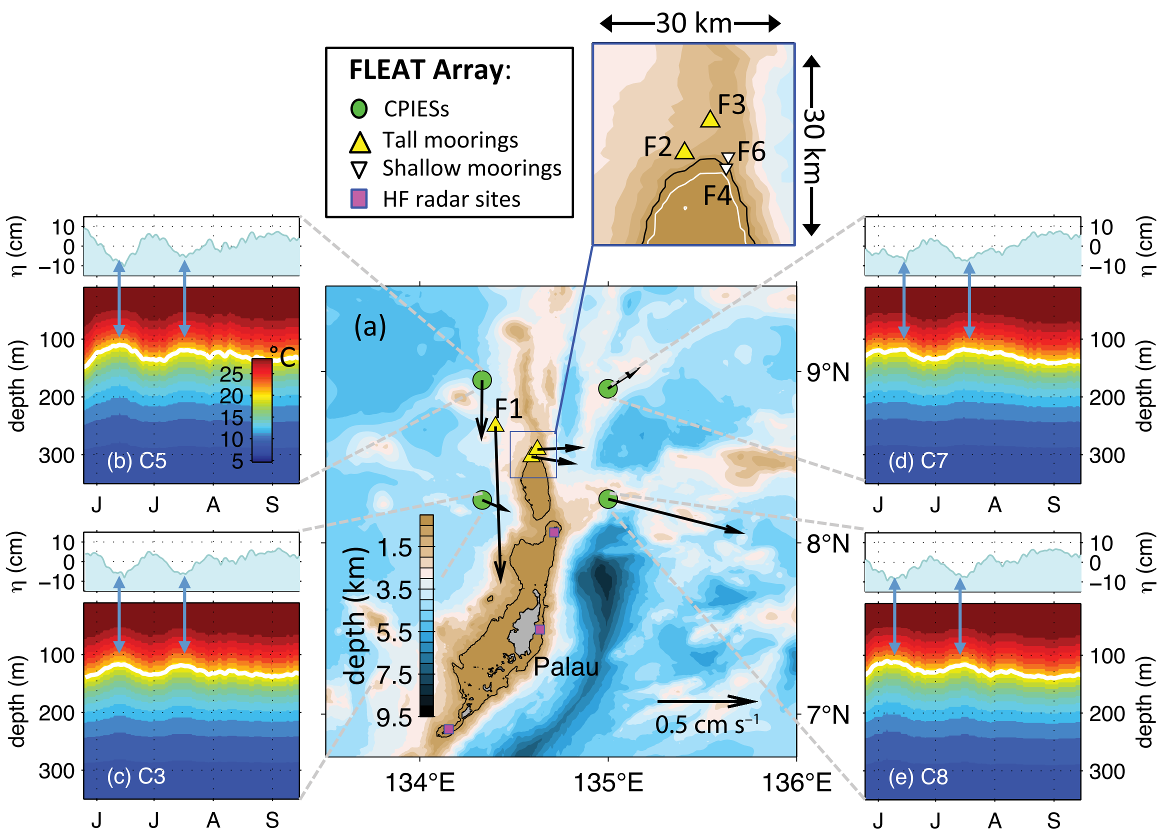

FIGURE 2. Maps and measurements from the FLEAT Array. (a) Map of Palau showing components of the FLEAT Array, with a close-up of the instrument sites at the tip of Velasco Reef (square enclosure). Bottom depth is shaded with the 500 m isobath contoured (black). Near the steep edge of Velasco Reef, the 50 m isobath is also indicated (white). Arrows show the 10-month averages of deep velocities measured ~50 m above the bottom. For each CPIES site, panels (b–e) show the first four months of the time series of SSH anomaly (η, top) and of temperature profiles (bottom). These are inferred from CPIES bottom pressure and acoustic travel time records using a lookup table generated for the region from more than 7,000 dives with Spray gliders (the methods used here are as in Mensah et al., 2016, and Andres et al., 2017). Superimposed on each temperature-profile time series is the depth of the σ_θ = 24.5 kg m^3 isopycnal surface (white contour), also inferred from the respective acoustic travel time records. During this four-month time period, two cyclonic eddies arrived at the array and caused the sea surface to fall and the thermocline to heave at each CPIES site. The extrema in sea surface height and thermocline depth were reached in mid-June and mid-July (as indicated with the double arrows). Observations made at the shallow mooring sites, F6 and F4 (small white triangles), are included in the supplementary materials.

mirrored by a shallower thermocline observed in the glider profiles near Palau (Figure 3c), the patterns of SSH gradients during both time spans are broadly similar (Figure 3a and b, white contours) and consistent with a westward-flowing NEC. Drifters released during each period corroborate this persistent flow pattern. Both drifters are initially swept westward in the NEC, entrained into the southward flowing Mindanao Current and then returned eastward along the northern edge of the NECC. In the former (El Niño) case, the drifter is swept northward and loops back into the NEC and the Mindanao Current after passing along the western edge of Palau. In the latter (La Niña) case, the drifter is caught in a semi-permanent circulation (visible both in the drifter track and the SSH pattern) on the southeastern edge of Palau.

With time-mean deep flows that oppose these upper-ocean currents in mind, we next examine whether mesoscale eddies that passed through the FLEAT Array influenced the deep velocity field around the ridge.

MESOSCALE EDDIES: WHAT'S GOING ON BENEATH THE SURFACE?

Near-surface signals associated with mesoscale eddies are evident as highs and lows in SSHa maps from altimetry (e.g., Figure 1) or as regions of positive and negative relative vorticity (Figure 4) derived from the near-surface geostrophic velocity field, which is, in turn, estimated from the SSH gradients. Because the altimeter measurements have relatively coarse temporal and horizontal resolution and also cannot "see" below the near-surface layer, they cannot resolve the details of mesoscale eddies' interactions with the topography around Palau. The FLEAT in situ data can fill in some of these gaps by providing information about the sea surface at better temporal and horizontal resolution than altimetry, and by providing information about the thermocline and deep currents. We use the CPIES observations to examine the eddies in the "far field" around the Kyushu-Palau Ridge.

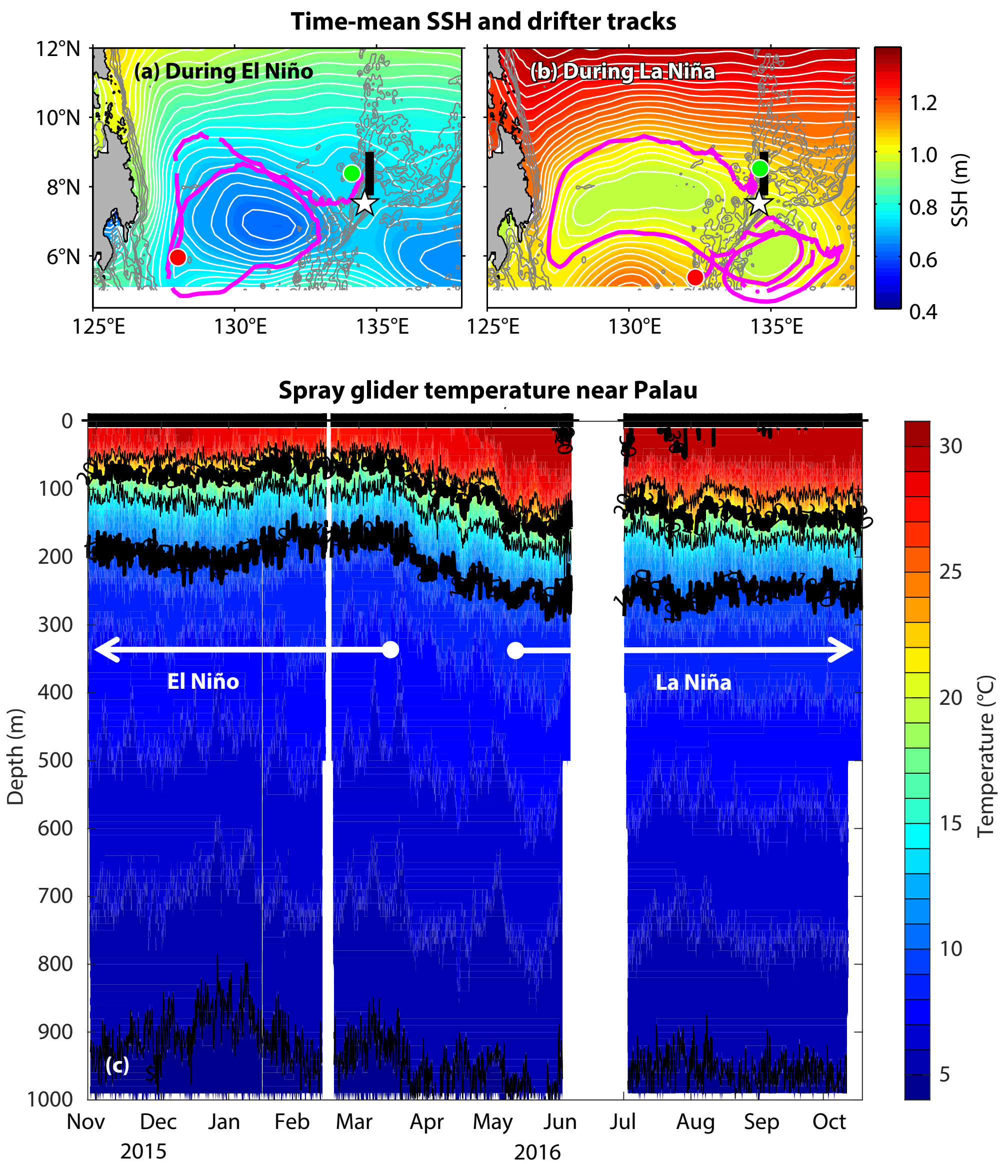

FIGURE 3. Temporal and spatial context for the FLEAT Array obtained from altimetry and drifters (panels a and b) and gliders (panel c). Panels (a) and (b) indicate the upper-ocean flow as inferred from the SSH field and drogued drifters during two different time periods, each lasting several months, that bracket the 10-month FLEAT Array deployment period. Panel (a) is the time-averaged SSH (shading and white contours) from satellite altimetry for the period October 19, 2015–January 11, 2016, when the region was in an El Niño state. The magenta curve is the trajectory of a drogued drifter during the same three-month period, with the track beginning at the green dot and ending at the red dot. Panel (b) is as in (a), but for the period May 23, 2017–October 5, 2017, when the region was in a La Niña state and another drifter (magenta) was tracked through the region. In both panels, bathymetry contours are highlighted at 1,000 m increments from 1,000 m to 4,000 m depths (gray), SSH is contoured at 1 cm increments (white), and the white star indicates the location of Palau. In (a) and (b) the black line is a repeat glider track for the Spray glider temperature profiles shown in (c) for the time period October 2015 through October 2016, which spans the El Niño/La Niña transition. This track is just to the west of the Kyushu-Palau Ridge. Notably, the thermocline is about 50 m deeper after the El Niño/La Niña transition, consistent with a higher sea level due to a greater steric contribution during the La Niña period (evident by comparing panels a and b).

To examine the eddies' vertical structure near the ridge, we use the tall moorings and the shallow moorings.

Sea Surface Height

At each CPIES site, the local time series of inferred sea surface height anomalies (η) can be obtained by combining the bottom pressure record with the acoustic travel time record (see the caption to Figure 5). Low-pass filtered records of these CPIES-derived measures (η) correspond quite well with the satellite-derived SSHa interpolated onto the CPIES locations (figure not shown). The most intense anomaly detected by the CPIES array was a drop in the (inferred) sea surface that began at the end of May (Figure 5). At the anomaly's peak expression (in mid-June), the sea surface was about 10 cm lower than the record average. Another sea surface drop, reaching to −8 cm, began about a month after the first and influenced the SSH around Velasco Reef and the Kyushu-Palau Ridge through the middle of August. These two sea surface lows, inferred from the in situ

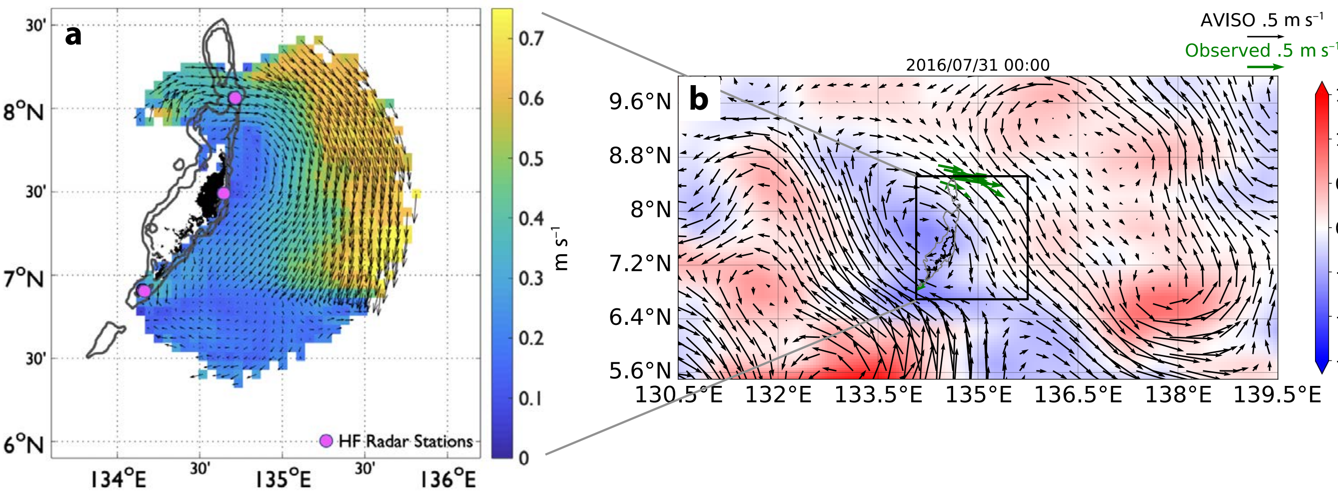

FIGURE 4 (above). Comparison of the velocities around Palau inferred in the near-field from HF radar (a) and in the far-field from satellite altimetry and the moorings (b). (a) Three-day (July 30–August 1, 2016) average surface velocities (arrows) and speeds (shading) as measured by land-based HF radar (station locations in pink). The northern portion of the radar domain captures the strong east and southeastward flow associated with the arrival of a cyclonic eddy. (b) Snapshot on July 31, 2016, of ζ/*f*, which is the relative vorticity (δ*v*/δx – δ*u*/δy) normalized by planetary vorticity (shading), where ζ is computed using absolute surface geostrophic velocities (*u*, *v*) from altimetry (black arrows). Green arrows show the 10-day low-pass filtered, surface-averaged (0–50 m) currents from the tall moorings. During the snapshot shown here, the northern tip of Palau is exposed to a southeastward geostrophic flow and is situated between positive and negative vorticity features associated with the arrival of an SSH low at the array (as shown in Figure 1c). In situ observations from the moorings capture the southeastward large-scale near-surface flow, and serve to validate, to first order, the velocity estimates from altimetry. These vorticity features, associated with the westward-propagating mesoscale eddies that manifest in SSH, tend to propagate westward across Palau (e.g., see an animation of panel b in the supplementary materials).

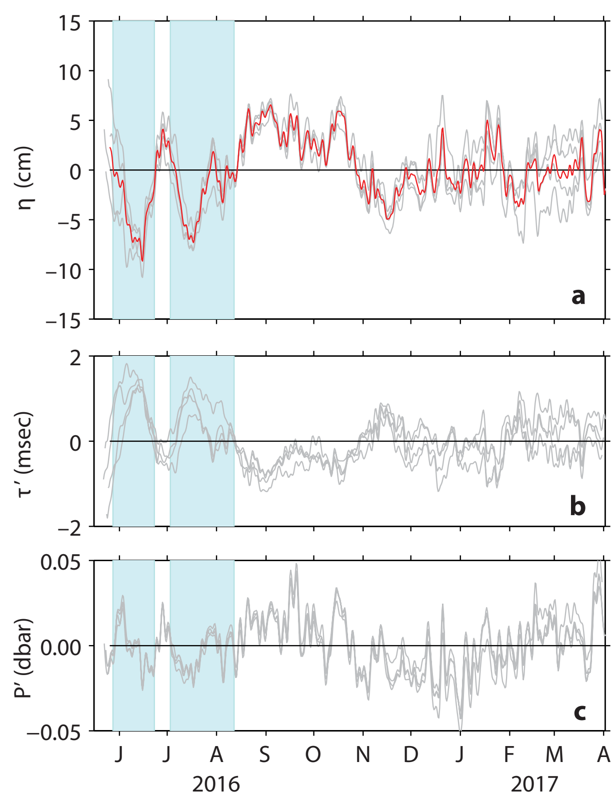

FIGURE 5 (right). Time series of the inferred (panel a) and measured (panels b and c) quantities from the CPIESs. Panel (a) shows η (the SSH anomalies inferred from the in situ measurements) at each of the four CPIES sites (gray curves) and averaged across the sites (red curve). These are calculated by combining each CPIES's three-day low-pass filtered records of bottom pressure anomaly: p′ (shown in panel c and used to obtain a mass loading contribution to SSH, η_{ML}) with the demeaned acoustic travel time records, τ′ (shown in panel b and from which the steric contribution to SSH, η_{ST}, can be inferred by using a look-up table to relate τ′ to geopotential anomaly, φ). The CPIES-inferred SSH anomaly (η) is the sum of the two components (Baker-Yeboah et al., 2009): $\eta_{ML} + \eta_{ST}$, where $\eta_{ML} = p'/\rho g$, and $\eta_{ST} = \varphi/g$. Here, ρ is the bottom density, *g* is acceleration due to gravity, and φ is the lookup-table inferred specific volume anomaly integrated between a reference level and the surface. Comparing the τ′ and p′ records, the eddies' expressions (highlighted with cyan shading) are more pronounced in τ′ than in p′, consistent with a large steric contribution to η (and a relatively small mass loading contribution) as these mesoscale eddies propagate across the Kyushu-Palau Ridge.

CPIES measurements, correspond to the arrivals from the east of two SSH lows evident in sequences of altimetry maps (Figure 1). The features in the altimetry SSHa maps are large, each about 350 km in diameter (by comparison, Palau is only about 60 km long and the CPIES spacing is about 70 km).

Thermocline Displacements

In data from the 10-month FLEAT experiment, the thermocline (or pycnocline) near Palau is quite shallow, averaging about 130 m depth (see the white curves in Figure 2b–e). Using the CPIES-measured acoustic travel time records with a lookup table to infer temperature (or density), the time-dependent depth of the thermocline (or pycnocline) can be estimated to examine the subsurface influence of mesoscale eddies. The FLEAT CPIES records show that, to first order, as mesoscale eddies pass through the array, the depth of the thermocline mirrors that of the sea surface: sea surface lows are accompanied by a shallower thermocline, and sea surface highs are accompanied by a deeper thermocline. During the passage of the two cyclonic eddies through the FLEAT Array, the sea surface lows (reaching to about −10 cm and −8 cm) are accompanied by displacements that heave the thermocline by about 16 m and 12 m, respectively (where the effect of each eddy has been averaged across the four sites).

Near-Bottom Currents

Bottom depths at the four CPIES sites are quite deep (ranging between 2,600 m and 4,300 m), and not surprisingly, like the time-means, the time-varying bottom currents measured here are, in general, very weak. Nevertheless, mesoscale signals in the upper ocean are accompanied by deep expressions, evident both in the low-pass filtered bottom pressure records (Figure 5c) and in the near-bottom currents. The passages of the two cyclonic eddies are detectable in the measured currents at all sites except C8 (Figure 6, cyan shaded times), which seems to be shielded from the effects of mesoscale eddies. Perhaps this has to do with the topography, as C8 sits on the southern flank of a deep spur that juts eastward from Palau and Velasco Reef.

OVER THE RIDGE

For a more detailed view of the flow close to the Kyushu-Palau Ridge, we next turn to the tall moorings to examine the vertical structure of the horizontal currents where the eddies were directly encountering topography. While the tall moorings, which were deployed a few weeks after the CPIESs, did not quite capture all of the first cyclonic eddy, they were in the water in time to fully sample the passage of the second cyclonic eddy over the ridge, so we focus on this event in the CPIESs records (Figure 6, the second cyan shaded period) and in the tall-mooring records (Figure 7 and supplementary materials, the time span denoted with the green vertical lines).

The CPIES-derived η (Figure 5, inferred from bottom pressure and acoustic travel time) and directly measured bottom currents (Figure 6) suggest that this second cyclonic eddy is equivalent barotropic (that is, the deep currents—though weak—seem to be going the same way as the upper ocean flow, with cyclonic circulation around the SSH low both in the upper ocean and in the deep ocean). This interpretation for the second eddy seems consistent across sites C3, C5, and C7 (and as noted before, at C8 there is no detectable deep expression of the eddy, even though it is present in the η time series—possibly due to shadowing

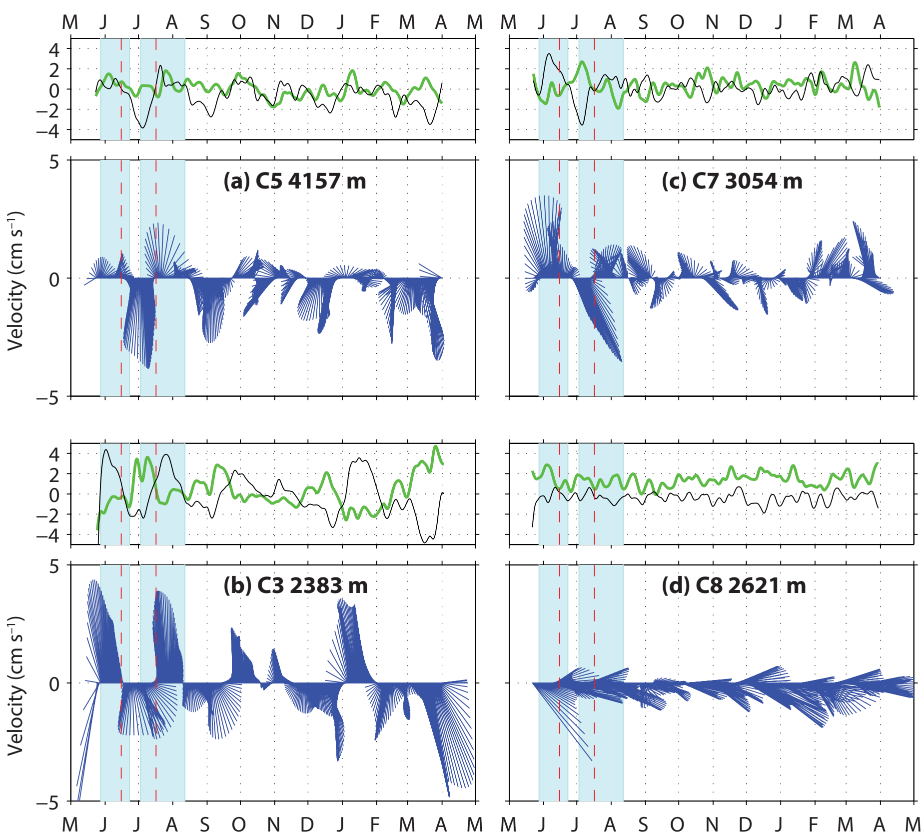

FIGURE 6. Ten-day, low-pass filtered currents measured 50 m off the bottom at the four CPIES sites shown as time series of stick plots (dark blue, with up indicating north) and decomposed into the meridional (thin black) and zonal (thick green) components. The cyan shaded regions indicate the times (based on η and thermocline displacements) when the two cyclonic eddies were affecting the upper ocean within the FLEAT Array (May 28–June 23 and July 3–August 12). Red vertical lines indicate the times of maximum η displacement for each eddy (from the spatial average across sites, i.e., the red curve in Figure 5), which can be thought of as the time when the eddy-eye is passing overhead. Bottom depths at each site are indicated.

by the spur in the topography).

In contrast to this suggestion of equivalent barotropic flow away from the Kyushu-Palau Ridge, the ADCP-measured velocities at the tall mooring sites suggest a more complicated layered flow structure close to the ridge at the tip of Velasco Reef. Consistent with the η signals at the CPIES sites, this July/August eddy is one of the strongest near-surface features in each of the tall mooring's ADCP records (Figure 7 and supplementary materials); however, in contrast to the CPIESs measurements, this feature doesn't seem to be a simple equivalent barotropic cyclonic eddy swirling around a sea surface low. Just north of Velasco Reef, at sites F2 and F3 on the western flank of the Kyushu-Palau Ridge, the strongest flows are in the upper ocean, with strong shear between the surface and ~100 m depth (which corresponds with the nominal thermocline depth here). Beneath this is a thick layer of counter-rotating flow (from ~100 m to ~1,000 m depth, with the most intense flow around 500 m). Below this, the flow reverses again. The nearby ridge crest rise to about 950 m depth and below this depth the eddy's deep-reaching currents likely directly come into contact with topography. Presumably, the eddy's vertical structure here is highly dependent on the details of the local topography with which the deep-reaching eddy is interacting. Notably, not only are the velocities in these deep layers that directly contact the topography affected by the interaction but also the velocities in the overlying layers above the ridge crest and above the thermocline.

A "TYPICAL" OR "SPECIAL" EVENT?

This July/August mesoscale eddy and its June predecessor were the strongest in the 10-month FLEAT records in terms of η (Figure 5), thermocline displacements (insets to Figure 2), and near-bottom currents at most of the CPIES sites (Figure 6). It is worth noting that this time period is just when the region was relaxing from a very strong El Niño to more neutral conditions. In the broader region around Palau, this relaxation manifested (1) in regional sea levels, which increased throughout the western tropical North Pacific (compare the SSH in panels a and b in Figure 3); (2) as changes in the upper-ocean's mean circulation—evidenced in the regions' SSH gradients, with less tightly packed SSH isopleths (implying weaker westward geostrophic flow north of Palau during the El Niño, Figure 3a) that transitioned to more tightly packed SSH isopleths (implying stronger westward flow north of Palau during La Niña, Figure 3b); and (3) in a deeper thermocline after the transition from the El Niño, as measured by a Spray glider flying continuously along a north-south transect west of Palau (Figure 3c).

While westward-propagating mesoscale eddies are not uncommon in the region (e.g., see the maps in Chelton et al., 2011), the strong cyclonic eddies sampled by the FLEAT Array and discussed here may be specifically related to the ocean's response to the termination of the El Niño via intraseasonal oscillations as described in Schönau et al. (2019, in this issue). It will require further study of more eddies to assess whether the subsurface characteristics of the eddies captured here during the end of the transition are unusual or are typical of the region's mesoscale eddies.

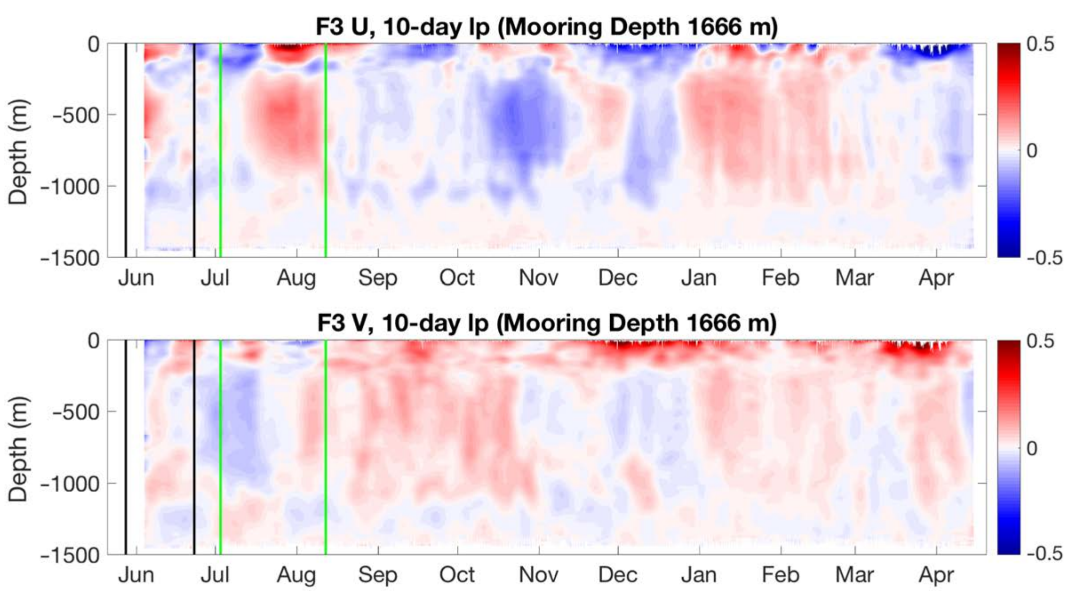

FIGURE 7. Zonal (top) and meridional (bottom) currents (m s^{-1}, shaded) 10-day low-pass filtered as measured at site F3 at the northern edge of Velasco Reef from June 2016 through April 2017. The vertical black lines bracket the timespan when the first cyclonic eddy was passing through the FLEAT Array (though the CPIESs were deployed by this point, the tall moorings were not yet all in the water). The vertical green lines bracket the time span when the second cyclonic eddy was sampled by the FLEAT Array. This feature is also evident in the velocity profile time series for each of the other tall mooring sites (see the supplementary materials).

SUPPLEMENTARY MATERIALS

Supplementary Figures S1–S4 are available online at https://doi.org/10.5670/oceanog.2019.410. The Supplemental Video is available on The Oceanography Society YouTube channel at https://youtu.be/WlpmJK43VzE.

REFERENCES

Aleynik, D., M.E. Inall, A. Dale, and A. Vink. 2017. Impact of remotely generated eddies on plume dispersion at abyssal mining sites in the Pacific. *Scientific Reports* 7, https://doi.org/10.1038/s41598-017-16912-2.

Andres, M., V. Mensah, S. Jan, M.-H. Chang, Y.-J. Yang, C.M. Lee, B. Ma, and T.B. Sanford. 2017. Downstream evolution of the Kuroshio's time varying transport and velocity structure. *Journal of Geophysical Research* 122: 3,519–3,542, https://doi.org/10.1002/2016JC012519.

Baker-Yeboah, S., D.R. Watts, and D. Byrne. 2009. Measurements of sea surface height variability in the eastern South Atlantic from pressure-sensor equipped inverted echo sounders: Baroclinic and barotropic components. *Journal of Atmospheric and Oceanic Technology* 26(12):2,593–2,609, https://doi.org/10.1175/2009JTECHO659.1.

Chelton, D.B., M.G. Schlax, and R.M. Samelson. 2011. Global observations of nonlinear mesoscale eddies. *Progress in Oceanography* 91(2):167–216, https://doi.org/10.1016/j.pocean.2011.01.002.

Jan, S., V. Mensah, M. Andres, M.-H. Chang, and Y.J. Yang. 2017. Eddy-Kuroshio interactions: Local and remote effects. *Journal of Geophysical Research* 122:9,744–9,764, https://doi.org/10.1002/2017JC013476.

Mensah, V., M. Andres, R.-C. Lien, B. Ma, C.M. Lee, and S. Jan. 2016. Combining observations from multiple platforms across the Kuroshio northeast of Luzon: A highlight on PIES data. *Journal of Atmospheric and Oceanic Technology* 33:2,185–2,283, https://doi.org/10.1175/JTECH-D-16-0095.1.

Merrifield, S.T., P.L. Colin, T. Cook, C. Garcia-Moreno, J.A. MacKinnon, M. Otero, T.A. Schramek, M. Siegelman, H.L. Simmons, and E.J. Terrill. 2019. Island wakes observed from high-frequency current mapping radar. *Oceanography* 32(4):92–101, https://doi.org/10.5670/oceanog.2019.415.

Johnston, T.M.S., M.C. Schönau, T. Paluszkiewicz, J.A. MacKinnon, B.K. Arbic, P.L. Colin, M.H. Alford, M. Andres, L. Centurioni, H.C. Graber, and others. 2019. Flow Encountering Abrupt Topography (FLEAT): A multiscale observational and modeling program to understand how topography affects flows in the western North Pacific. *Oceanography* 32(4):10–21, https://doi.org/10.5670/oceanog.2019.407.

Ramp, S., J.A. Colosi, P.F. Worcester, F.L. Bahr, K.D. Heaney, J.A. Mercer, and L.J. Uffelen. 2017. Eddy properties in the subtropical countercurrent, Western Philippine Sea. *Deep Sea Research Part I* 125:11–25, https://doi.org/10.1016/j.dsr.2017.03.010.

Rudnick, D.L., K.L. Zeiden, C.Y. Ou, T.M.S. Johnston, J.A. MacKinnon, M.H. Alford, and G. Voet. 2019. Understanding vorticity caused by flow passing an island. *Oceanography* 32(4):66–73, https://doi.org/10.5670/oceanog.2019.412.

Schönau, M.C., and D.L. Rudnick. 2015. Glider observations of the North Equatorial Current in the western tropical Pacific. *Journal of Geophysical Research* 120:3,586–3,605, https://doi.org/10.1002/2014JC010595.

Schönau, M.C., H.W. Wijesekera, W.J. Teague, P.L. Colin, G. Gopalakrishnan, D.L. Rudnick, B.D. Cornuelle, Z.R. Hallock, and D.W. Wang. 2019. The end of an El Niño: A view from Palau. *Oceanography* 32(4):32–45, https://doi.org/10.5670/oceanog.2019.409.

Sekine, Y. 1989. Topographic effects of a marine ridge on the spin-down of a cyclonic eddy. *Journal of the Oceanographical Society of Japan* 45:190–203, https://doi.org/10.1007/BF02123463.

Watts, D.R., and H.T. Rossby. 1977. Measuring dynamic heights with inverted echo sounders: Results from MODE. *Journal of Physical Oceanography* 7:345–358, https://doi.org/10.1175/1520-0485(1977)007<0345:MDHWIE>2.0.CO;2.

Yan, X., D. Kang, E.N. Curchitser, and C. Pang. 2019. Energetics of eddy–mean flow interactions along the western boundary currents in the North Pacific. *Journal of Physical Oceanography* 49(3):789–810, https://doi.org/10.1175/JPO-D-18-0201.1.

Yang, Q., M. Nikurashin, H. Sasaki, H. Sun, and J. Tian. 2019. Dissipation of mesoscale eddies and its contribution to mixing in the northern South China Sea. *Scientific Reports* 9, https://doi.org/10.1038/s41598-018-36610-x.

Zhang, Z., Y. Wang, and B. Qiu. 2014. Oceanic mass transport by mesoscale eddies. *Science* 345(6194):322–324, https://doi.org/10.1126/science.1252418.

Zhang, Z., J. Tian, B. Qiu, W. Zhao, P. Chang, D. Wu, and X. Wan. 2016. Observed 3D structure, generation, and dissipation of oceanic mesoscale eddies in the South China Sea. *Scientific Reports* 6, https://doi.org/10.1038/srep24349.

ACKNOWLEDGMENTS

We gratefully acknowledge the help of Captain David Murline and the crew of R/V *Roger Revelle* and the shore-based assistance of Lori Colin and Pat Colin of the Coral Reef Research Foundation. We sincerely thank Terri Paluszkiewicz for her steadfast support of basic research programs, including FLEAT, during her many years of service to the community as Office of Naval Research (ONR) Physical Oceanography Program Manager. MA was supported by ONR grant N000141612668, MS and MAM by N00014-16-1-2671, MHA and JAM by N00014-15-1-2264 and N00014-16-1-3070, GV by N00014-15-1-2592, DLR by N00014-15-1-2488, and STM and EJT by N00014-15-1-2304. VH and LC were supported by ONR grant N00014-15-1-2286 and NOAA GDP grant NA15OAR4320071. RCM was supported by the Postdoctoral Scholar Program at the Wood Hole Oceanographic Institution, with funding provided by the Weston Howland Jr. Postdoctoral Scholarship. We thank the Palau National Government for permission to carry out the research in Palau.

AUTHORS

Magdalena Andres (mandres@whoi.edu) is Associate Scientist, Woods Hole Oceanographic Institution, Woods Hole, MA, USA. **Mika Siegelman** is a PhD Candidate, School of Ocean and Earth Science and Technology, University of Hawaiʻi at Mānoa, Honolulu, HI, USA. **Verena Hormann** is Project Scientist, Scripps Institution of Oceanography, University of California San Diego (SIO-UCSD), La Jolla, CA, USA. **Ruth C. Musgrave** was Postdoctoral Scholar, Woods Hole Oceanographic Institution, Woods Hole, MA, USA, and is now Assistant Professor, Dalhousie University, Halifax, Nova Scotia, Canada. **Sophia T. Merrifield** is Assistant Project Scientist, **Daniel L. Rudnick** is Professor, **Mark A. Merrifield** is Professor, **Matthew H. Alford** is Professor, and **Gunnar Voet** is Assistant Project Scientist, all at SIO-UCSD, La Jolla, CA, USA. **Hemantha W. Wijesekera** is Oceanographer, Naval Research Laboratory, Stennis Space Center, MS, USA. **Jennifer A. MacKinnon** is Professor and **Luca Centurioni** is Researcher, SIO-UCSD, La Jolla, CA, USA. **Jonathan D. Nash** is Professor, College of Earth, Ocean and Atmospheric Sciences, Oregon State University, Corvallis, OR, USA. **Eric J. Terrill** is Director, Coastal Observing Research and Development Center, SIO-UCSD, La Jolla, CA, USA.

ARTICLE CITATION

Andres, M., M. Siegelman, V. Hormann, R.C. Musgrave, S.T. Merrifield, D.L. Rudnick, M.A. Merrifield, M.H. Alford, G. Voet, H.W. Wijesekera, J.A. MacKinnon, L. Centurioni, J.D. Nash, and E.J. Terrill. 2019. Eddies, topography, and the abyssal flow by the Kyushu-Palau Ridge near Velasco Reef. *Oceanography* 32(4):46–55, https://doi.org/10.5670/oceanog.2019.410.

COPYRIGHT & USAGE